

Numerical Simulation of Catastrophic Tsunami Propagation in the Indian Ocean (December 26, 2004)

A. I. Zaitsev¹, A. A. Kurkin¹, Corresponding Member of the RAS B. V. Levin², E. N. Pelinovsky³,
 A. Yalciner⁴, Yu. I. Troitskaya³, and S. A. Ermakov³

Received February 1, 2005

The December 26, 2004, Indian Ocean tsunami proved to be the most destructive one in the history of mankind: more than 150 000 people perished, and the economic damage inflicted amounted to billions of dollars. The tsunami had catastrophic effects in many countries of the Indian Ocean: Indonesia, Thailand, India, Sri Lanka, Maldives, Kenya, Somalia, and South Africa. Tsunami waves were recorded by tide gauges in the Indian, Atlantic, and Pacific Oceans. Gauges in the Russian Far East also recorded these waves (in particular, the height of tsunami waves in Severo-Kurilsk was 30 cm). The waves were also observed in space images. The source of the tsunami was a very strong earthquake ($M = 9$ on the Richter scale) whose epicenter was near the northern margin of Sumatra Island (3.298° N, 95.779° E). In the past 100 years, five earthquakes with as great or greater magnitude have been recorded: in the Aleutian (1946, $M = 9.3$; 1957, $M = 9.0$), Kamchatka (1964, $M = 9.0$), Chile (1960, $M = 9.4$), and Alaska (1964, $M = 9.1$ [1]). The earthquake epicenter and aftershocks are currently displayed on many Web sites (see, for instance, [2]; detailed information about the December 26, 2004, tsunami may also be found there). The present communication is devoted to the numerical simulation of tsunami propagation in the Indian Ocean, which has been undertaken in order to establish the trend of its orientation and calculate the distribution of wave heights along the coast.

To simulate tsunami propagation in the open ocean, we used an equation system of shallow water on the spherical Earth with allowance made for the Coriolis force.

$$\frac{\partial M}{\partial t} + \frac{1}{R \cos \theta} \frac{\partial}{\partial \lambda} \left(\frac{M^2}{D} \right) + \frac{1}{R \cos \theta} \frac{\partial}{\partial \theta} \left(\frac{MN \cos \theta}{D} \right) + \frac{gD}{R \cos \theta} \frac{\partial \eta}{\partial \lambda} = fN, \quad (1)$$

$$\frac{\partial N}{\partial t} + \frac{1}{R \cos \theta} \frac{\partial}{\partial \lambda} \left(\frac{MN}{D} \right) + \frac{1}{R \cos \theta} \frac{\partial}{\partial \theta} \left(\frac{N^2 \cos \theta}{D} \right) + \frac{gD}{R} \frac{\partial \eta}{\partial \theta} = fM, \quad (2)$$

$$\frac{\partial \eta}{\partial t} + \frac{1}{R \cos \theta} \left[\frac{\partial M}{\partial \lambda} + \frac{\partial}{\partial \theta} (N \cos \theta) \right] = 0, \quad (3)$$

where η is the water surface displacement, M and N are components of water discharge along latitude θ and longitude λ , $D = h(x, y) + \eta$ is the total water depth, $h(x, y)$ is the unperturbed depth, g is acceleration due to gravity, t is time, R is the Earth's radius, f is the Coriolis parameter ($f = 2\omega \sin \theta$), and ω is the rotation frequency of the Earth. Tsunami propagation in the coastal zone is simulated within the shallow-water system in Cartesian coordinates with allowance made for turbulent friction on the bottom (the influence of the Coriolis force is disregarded):

$$\frac{\partial M}{\partial t} + \frac{\partial}{\partial x} \left(\frac{M^2}{D} \right) + \frac{\partial}{\partial y} \left(\frac{MN}{D} \right) + gD \frac{\partial \eta}{\partial x} + \frac{k}{2D^2} M \sqrt{M^2 + N^2} = 0, \quad (4)$$

$$\frac{\partial N}{\partial t} + \frac{\partial}{\partial x} \left(\frac{MN}{D} \right) + \frac{\partial}{\partial y} \left(\frac{N^2}{D} \right) + gD \frac{\partial \eta}{\partial x} + \frac{k}{2D^2} N \sqrt{M^2 + N^2} = 0, \quad (5)$$

$$\frac{\partial \eta}{\partial t} + \frac{\partial M}{\partial x} + \frac{\partial N}{\partial y} = 0, \quad (6)$$

where k is coefficient of turbulent friction on the bottom ($k = 0.0025$). The numerical code was realized based on the TUNAMI software package, which was developed

¹ State Technical University, ul. Minina 24, Nizhni Novgorod, 603600 Russia; e-mail: kurkin@kis.ru

² Institute of Marine Geology and Geophysics, Far East Division, Russian Academy of Sciences, ul. Nauki 5, Yuzhno-Sakhalinsk, 693002 Russia; e-mail@lbw@imgg.ru

³ Institute of Applied Physics, Russian Academy of Sciences, ul. Ul'yanova 46, Nizhni Novgorod, 603950 Russia; e-mail: pelinovsky@hydro.app.sci-nnov.ru

⁴ Middle East Technical University, Ankara, 06531 Turkey; e-mail: yalciner@metu.edu.tr

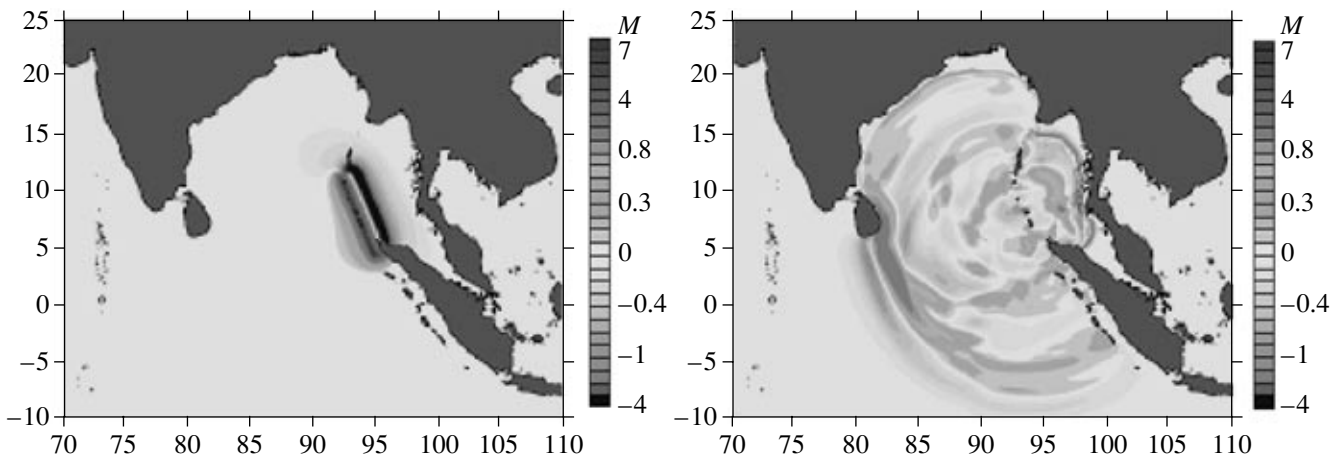


Fig. 1. Sealevel variations at the onset of the event (left) and after 2 h (right).

in Japan [3] and modified for computer calculations [4]. The conjugation of “spherical” and “flat” calculations in this package is described in [5]. Both models have been used previously for assessing tsunami risk in the Japan and Black Seas [6, 7]. Seafloor bathymetry data (GEBCO Digital Atlas, British Oceanographic Data Centre) was taken with a resolution of one angular minute (about 1.5 km). Wave roiling on the coast was not assessed, as this requires more detailed seafloor bathymetry and land topography. The schematization of the coast as a flat slope is somewhat equivalent to vertical wall at the last offshore point (at a depth of approximately 10–20 m), where the condition of complete reflection is assumed. The condition of free wave drift was assumed for marine boundaries between the Atlantic and Pacific oceans. Initial conditions (tsunami center) were chosen from the seismic model [8]. In particular, we prescribed the following earthquake parameters: fault length 666 km, width 90 km, focus depth 7 km, angle of pitch in the fault plane 340°, dip angle in the same plane 13°, angle of fault displacement 55°, and displacement 20 m. Such an earthquake provokes the initial dipole-type sealevel change with a maximal rise of 7.2 m and depression of 3.4 m.

Figure 1 illustrates results from the calculation of tsunami propagation in the Indian Ocean. It reveals instantaneous changes in sealevel immediately after the earthquake and 2 h later. The wave reached the coast of Thailand in approximately 1 h, India and Sri Lanka in 2 h, Somalia in 7 h, and South Africa in 12 h. The calculated values of tsunami wave arrival time are in good agreement with the calculation results based on the radial model [2] and observation data.

The spatial distribution of the maximal waterlevel rise in the ocean (directional diagram) is shown in Fig. 2. As expected, the tsunami provokes a strong rise of water on the coast nearest to the epicenter (Indonesia, Thailand, Malaysia, and Myanmar). High tsunami waves propagate toward Sri Lanka, Maldives, the

southern edge of India, and the African coast (the Republic of South Africa, Kenya, and Somalia). It was in these countries that the greatest loss was inflicted by tsunami, confirming forecasts based on the numerical model. It should be noted that other researchers have obtained analogous results based on the directional diagram. The distinction is related to different models of the source. The most adequate model will be chosen after all field data has been processed.

We have also calculated forms of tsunami waves (marigrams) at different points, and the results are presented on the web site [9]. According to these calculations, as a group of waves approaches the coast, the second or third wave is often the maximal one, which is in agreement with observation data. In Thailand, the tsunami begins with ebb tide, and this also complies with observations. The first tsunami representative to approach India is the wave crest, but it is not necessarily great as compared to the next wave trough, which can easily be taken as an initial ebb tide.

Figure 3 presents more detailed information on wave height along the coastal zone. In general, the wave height reaches 10 m at points near the epicenter (Indonesia and Thailand), the maximal height being 16 m in the north of Thailand. The wave height on the coasts of India and Sri Lanka reaches 6 m. As noted above, we did not consider wave roiling on the coast in our calculations. In shallow-water areas, the wave can be 2–3 times higher (see, for example, [10]) or even more in some places. This satisfactorily explains the anomalously high splashes observed on the coasts. There are currently several international and national expeditions inspecting traces of tsunami along the coast of the Indian Ocean (this investigation may take several months). The data obtained will be used for more detailed correlation and refinement of the tsunami source model. Some of the data (e.g., satellite photographs) is already available. Figure 4A presents images of the southern coast of the Hindustan Peninsula (8°01' N

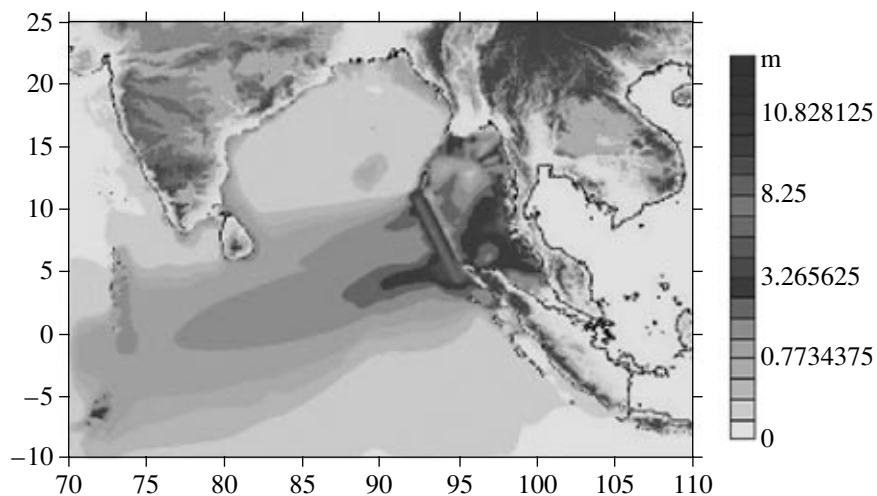


Fig. 2. Directional diagram of tsunami waves in 2004 in the Indian Ocean.

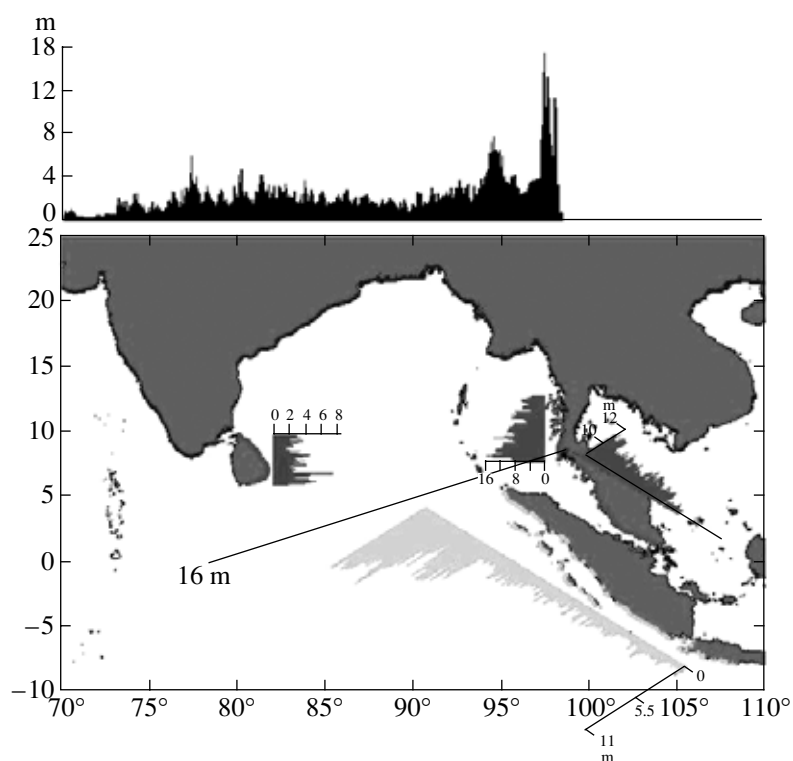


Fig. 3. Distribution of the maximal sealevel rise along the coast of the Indian Ocean.

and $77^{\circ}11' E$). Figure 4B shows the western coast of the Indochina Peninsula at a location approximately 60 km southeast of Phuket Island ($8^{\circ}01' N$, $99^{\circ}08' E$). These images were obtained by means of the optical system of the SPOT-4 Satellite on December 26, 2004 (see [11]). As is evident from the automatically recorded times shown in Fig. 4, image A was obtained 4 h 44 min after the earthquake, whereas image B was recorded 3 h 22 min after the earthquake. These time records are consistent

with the calculated arrival times of tsunami waves and with witness reports. Image A, which was obtained during the tsunami event, shows a zone of intense wave collapse east of the settlement at Colachel (this zone was not observed in the photograph taken on December 16, 2004, prior to the wave arrival), as well as a system of bands with a characteristic scale varying from 5 to 15 km. Such a distribution of bands qualitatively corresponds to the arrangement of fronts of long surface

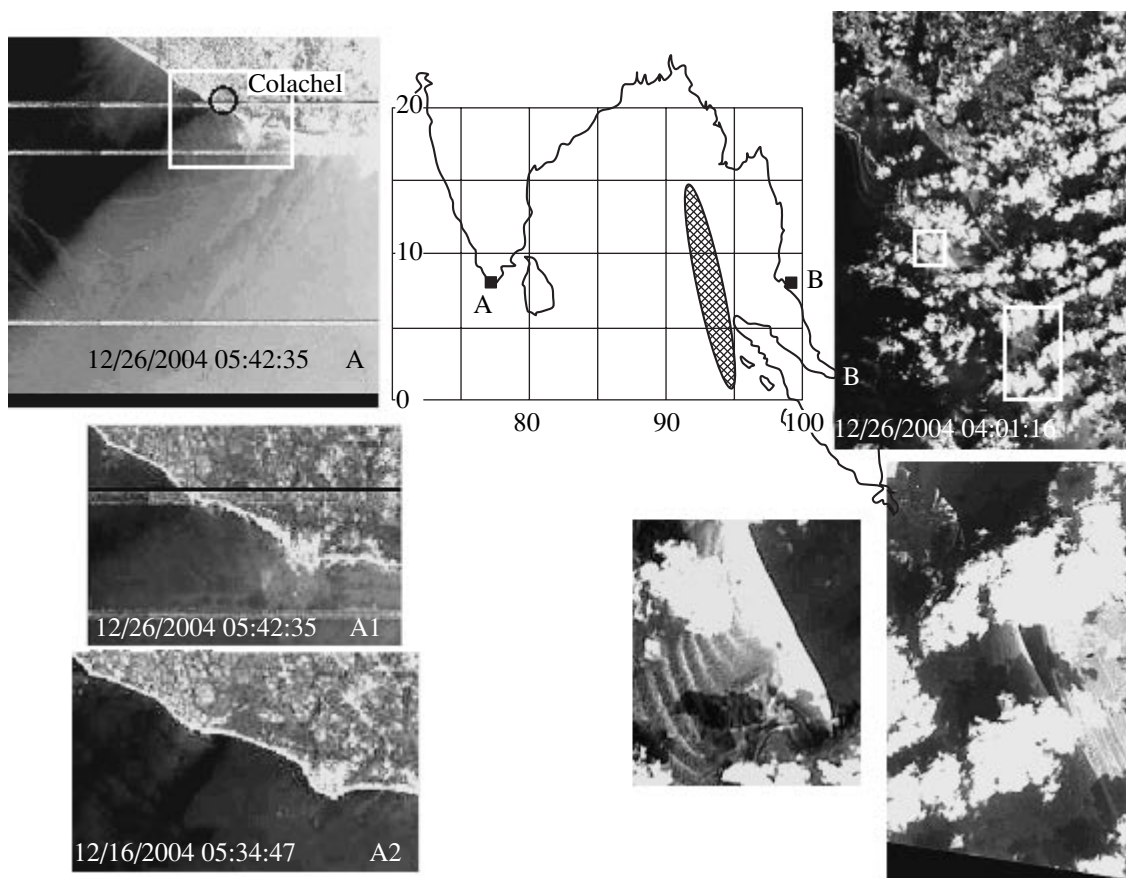


Fig. 4. Space images A [11] and B [12] of tsunami.

waves with consideration for refraction on the nonuniform bottom.

In conclusion, we should point out that, although the Indian Ocean has traditionally been regarded as a low risk region in terms of tsunami, approximately 30 tsunami events are known for this region in the history of mankind. Several strong tsunamis have occurred in this region in the past 150 years [13]. For example, tsunami was recorded in the Arabian Sea after the strong earthquake of 1945 ($M = 8$). Waves in Pakistan and India were rather high (3–15 m). The tsunamis in 1977 and 1994 on the coast of Indonesia provoked waves as high as 3 m and they reached the western coast of Australia in a few hours. Worthy of special consideration is the tsunami caused by the eruption of the Krakatau Volcano in 1883. The wave was as high as 45 m in the Sunda Strait (Indonesia) and was responsible for the loss of 36 000 people. This tsunami also had a global (although not catastrophic) impact and was felt in many countries of the Indian Ocean (India, Pakistan, Sri Lanka, Yemen, the Republic of South Africa, and the Mascarene Islands). It was registered worldwide by numerous tide gauges (the total number of marigrams available is 35). In [14], the global character of the 1988 tsunami has been simulated based on the 2004 tsunami model. The

occurrence of two global and several regional tsunami waves in the Indian Ocean indicates the need for the creation of an international tsunami warning system and compilation of the tsunami hazard map for this region. Numerical calculations of tsunami wave propagation would be an integral part of assessing the comparative security of different coastal areas in the Indian Ocean.

ACKNOWLEDGMENTS

This work was supported by the Russian Foundation for Basic Research (project nos. 03-05-64975, 04-05-64264, 05-05-64137, and 05-05-64265), INTAS (project nos. 01-2156 and 03-51-4286), and the Foundation for the Support of Leading Scientific Schools (NSH-2104.2003.5).

REFERENCES

1. K. Abe, *J. Geophys. Research* **84**, 1561 (1979).
2. V. K. Gusakov, <http://tsun.sccc.ru/tsulab/20041226.htm>.
3. C. Goto, Y. Ogawa, N. Shuto, and N. Imamura, *Numerical Method of Tsunami Simulation with the Leap-Frog Scheme (IUGG/IOC Time Project) IOC Manual* (UNESCO, Paris, 1997), No. 35.

4. A. A. Kurkin, A. I. Zaitsev, A. Yalciner, and E. N. Pelinovsky, *Izv. Ross. Akad. Nauk, Ser. Prikl. Matem. Mekh.*, No. 9, 88 (2004).
5. A. A. Kurkin, E. N. Pelinovsky, B. H. Choi, and J. S. Lee, *Okeanologiya* **44**, 179 (2004).
6. A. Yalciner, E. Pelinovsky, T. Talipova, *et al.*, *J. Geophys. Res.* **109** (C12), C12023 10.1029/2003JC002113 (2004).
7. B. N. Choi, E. Pelinovsky, S. J. Hong, and S. B. Woo, *Pure and Appl. Geophys.* **160**, 1383 (2003).
8. Y. Okada, *Bull. Seismol. Soc. Am.*, No. 75, 1135 (1985).
9. A. Yalciner, T. Tayamaz, U. Kuran, *et al.*, *The Model Studies on December 26, 2004, Indian Ocean Tsunami*, <http://yalciner.ce.metu.edu.tr/sumatra/simulations/index.htm>.
10. E. N. Pelinovsky, *Hydrodynamics of Tsunami Waves* (IPF RAS, Nizhni Novgorod, 1996) [in Russian].
11. *Spot Image Online Catalogue*, <http://sirius.spotimage.fr/>.
12. Centre for Remote Imaging, Sensing and Processing (CRISP) of the National University of Singapore, <http://crisp.nus.edu.sg/tsunami/tsunami/html>.
13. T. Murty and M. Rafiq, *Natur. Hazards*, No. 4, 81 (1991).
14. B. N. Choi, E. Pelinovsky, K. O. Kim, and J. S. Lee, *Natur. Hazards Earth System Sci.* **3**, 321 (2003).